

The low temperature co-fired ceramics (LTCC) chip for polymerase chain reaction (PCR) application

PAWEŁ BEMBNOWICZ^{1*}, PIOTR HERBUT¹, MAŁGORZATA MAŁODOBRA², ANNA KARPIEWSKA², LESZEK J. GOLONKA¹, ANNA JONKISZ², TADEUSZ DOBOSZ²

¹Wrocław University of Technology, Faculty of Microsystem Electronics and Photonics,
Janiszewskiego 11/17, 50-372 Wrocław, Poland

²Molecular Technique Unit, Silesian Piast Medical University,
ul. Marii Skłodowskiej-Curie 52, 50-369 Wrocław, Poland

*Corresponding author: pawel.bembnowicz@pwr.wroc.pl

The DNA (deoxyribonucleic acid) amplification chip made of DP951 (from DuPont) ceramics consists of a microchamber, internal and external metallization. The external metallization is used for attachment of SMD (surface mount device) electronics elements. The internal metal layer improves thermal conditions inside the chamber. The temperature distribution in the chamber is verified by numerical simulation. Heating is realized by an external SMD resistor. The temperature measurements are made by attached Pt100 component. The temperature control is realized by a microcontroller based electronic system. Settings and visualization of the polymerase chain reaction (PCR) process parameters are actualized by dedicated PC (personal computer) software. The system is successfully tested. The DNA amplification inside the low temperature co-fired ceramics (LTCC) chip is achieved.

Keywords: low temperature co-fired ceramics (LTCC), deoxyribonucleic acid (DNA), polymerase chain reaction (PCR).

1. Introduction

The ceramics has a wide range of applications. On the one hand, it is used in medicine as biomaterial, on the other, it is applied in electronics as an integrated package. There are alumina parts (*e.g.*, orthopedic or dental implants) which exist inside human body for several years without any sign of toxicity [1]. Since the 1980s the LTCC (low temperature co-fired ceramics) has been used in electronics for manufacturing of multilayer substrates. The technology enables the integration not only of conductor paths but also electronics components such as resistors [2] or capacitors. Since the middle 1990s low temperature co-fired ceramics has been used as a base material for microsystems. The multilayer technology enables the construction of three-dimen-

sional microfluidic channels and chambers [3]. The condition inside the structure can be monitored by buried integrated sensors (*e.g.*, temperature, humidity or gas sensor). Rapid development of analytic microsystems began in the last decade. Then, the LTCC was used for construction of micromixers [4, 5], the structure for capillary [6, 7] or gel electrophoresis [8] *etc.*

When the information about the first LTCC chip for chemical application was published, the scientists have started investigations on chemical resistivity of the ceramics. For example, this material was exposed to aggressive acids and bases [4, 5, 9]. The fired LTCC consists mainly of alumina (outstanding chemical resistivity) and glass (high chemical resistivity). Thus the resistance as high as the resistivity of borosilicate glass was expected. The results of tests confirmed the above thesis. The LTCC had a good chemical resistance against solvents. NaOH was the most destructive chemical solution for this ceramics according to the experiment. Both alumina and glass were corroded. Nevertheless, the LTCC proved to be a material with high chemical resistivity.

This is an important feature for chemical and biochemical reactors. The material of the structure cannot affect biochemical processes. The more sophisticated reaction mixture, the more probable that some of ingredients will react with the structure.

A PCR (polymerase chain reaction) is a process where specific fragments of DNA can be amplified. Prototype microstructures for the PCR reaction are widely described in literature [10]. However, none of them was commercially produced. There is still a place for improvement. Some types of LTCC are PCR-friendly and can be used for PCR microchip construction according to previous work [11] and literature [5]. Moreover, a successful PCR process in LTCC continuous flow chip has been reported [12].

In this paper, the further research [11] on LTCC PCR microreactor is reported. A process of designing and fabrication of an integrated ceramic chip is described. The numerical simulation of temperature distribution inside the structure is presented. The dedicated temperature management system is applied. The biological tests inside the LTCC structure are described.

2. Motivations

The LTCC material as a composition of glass and alumina is characterized by thermal conductivity equal to $3 \text{ Wm}^{-1}\text{K}^{-1}$. It makes it possible to construct structures where a high gradient of temperature can be observed [13, 14]. But a microchamber PCR reactor should have a low gradient of temperature. Moreover, the PCR is a process where the proper temperature management is a key to success. Numerical calculations are often applied in order to achieve proper temperature distribution inside PCR microstructures [15].

The LTCC technology enables conductive and resistive component integration. Usually, the passive electronic components are defined in a screen printing process. The components can be used as a buried heater and sensor. However, it is impossible

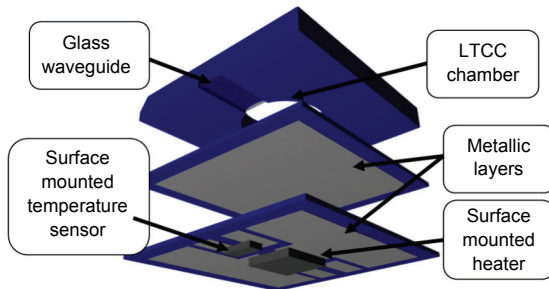


Fig. 1. Scheme of LTCC microchamber connected with SMD resistors.

to fabricate thick-film components with strictly defined resistance without post process trimming. The trimming process for low volume production is expensive and time consuming.

In the presented work, this problem was solved by using commercially available trimmed SMD (surface mount device) components. The SMD resistors are fabricated in high volume production. Thus, they are relatively cheap. Only metal conductive films were screen printed. In the previous article [11], a ceramic PCR microchamber with an external heating/cooling system was described. However, the heater and temperature sensor integration with LTCC chip is needed for higher system miniaturization (Fig. 1). The standard SMD resistor (1206 package) and Pt100 element (0805 package) can be soldered to the developed LTCC structure. In this case, the resistor works as a heater and Pt100 element is a temperature sensor. The additional buried element with high thermal conductivity can improve thermal property of the structure. A metallic layer can be applied in order to achieve uniform temperature distribution.

3. Numerical simulations and measurement of temperature distribution

An ANSYS[®] simulation software was applied for investigation of buried layers with high thermal conductivity which influences the temperature distribution inside the chamber [16]. The software uses finite element method (FEM) to make calculations

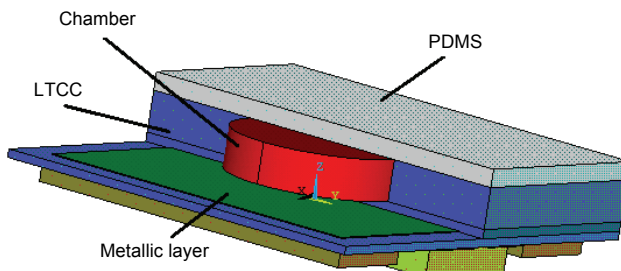


Fig. 2. The cross-sectional scheme of simulated structure.

of thermal fields. The chip model (Fig. 2) was built. The following simplified assumptions were made in the simulations:

- materials used in the project were isotropic and uniform in time and space,
- the device was placed in horizontal position and the heater and temperature sensor were mounted on the bottom side,
- the chamber was filled with water and a mechanism of convective heat transfer in the water was neglected,
- the chamber was sealed with PDMS layer,
- the heating was a result of current flow through the heating resistor (Joule heat),

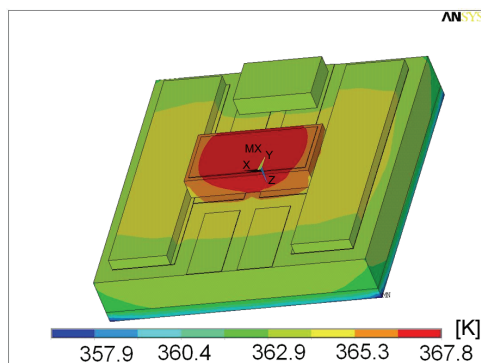


Fig. 3. Temperature distribution on the bottom side of the structure.

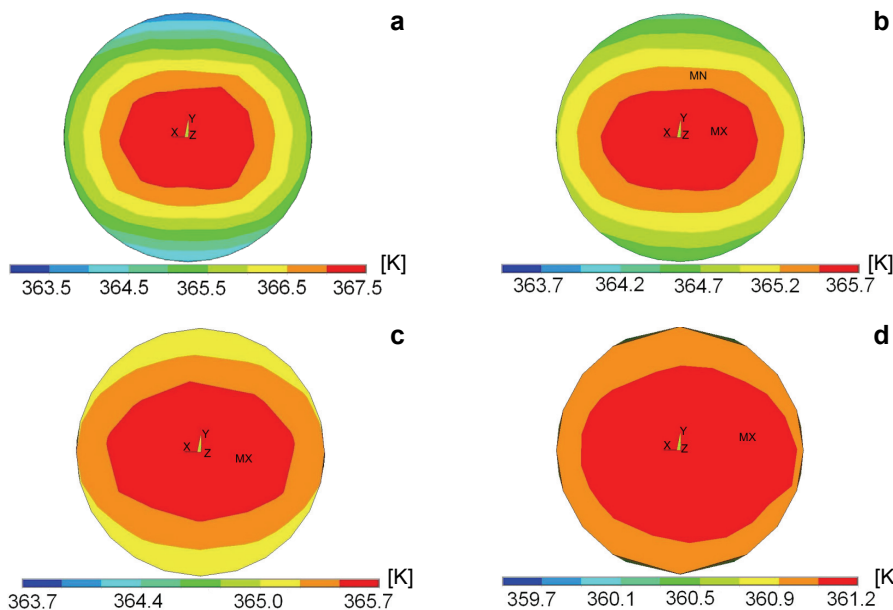


Fig. 4. Temperature distribution on the bottom of reaction chamber for: none buried metallic layer (**a**), one buried metallic layer (**b**), two buried metallic layers (**c**), three buried metallic layers (**d**). A diameter of the investigated area is 3 mm.

- heat loss from the structure took place through convection, which was modeled by applying the proper boundary condition on the outer surfaces of solid,
- radiation of thermal energy was neglected because of its weak influence on cooling process in comparison to convection,
- the heating was realized by applying the voltage boundary condition to the heating resistor.

The simulations of coupled thermoelectric fields were conducted. The applied material consisted of elements with 6 nodes, 8 walls and 2 degrees of freedom (DOF) – temperature and voltage.

A temperature distribution on the bottom side of the structure is shown in Fig. 3. The uniformity of the temperature on the bottom of the chamber and the influence of the number of buried metallic layers were investigated. The results are presented in Fig. 4.

The obtained result proved that applying of buried metallic layers improved the temperature uniformity on the bottom of the reaction chamber. The reduction of difference between maximum and minimum temperature on the bottom of the chamber from 4 °C to 0.37 °C (Fig. 5) was achieved by changing the number of metallic layers from 0 to 3. However, even one metal layer reduces the temperature difference to approximately 1.5 °C.

A construction with one buried metallic layer was chosen. More layers increase thermal mass of the structure and therefore increase the heating and cooling time during PCR process. Additionally, the temperature difference between the chamber and temperature sensor was examined. The difference between chamber's temperature and sensor's temperature was about 3 °C in the model with one metallic layer. This piece of information was taken into consideration during the sensor calibration.

The test structures were manufactured. They consisted of two LTCC layers (254 µm thick). A pattern which allowed SMD resistors soldering was printed on the first layer. A large metal pad was placed on the second layer. A DP6146 ink was

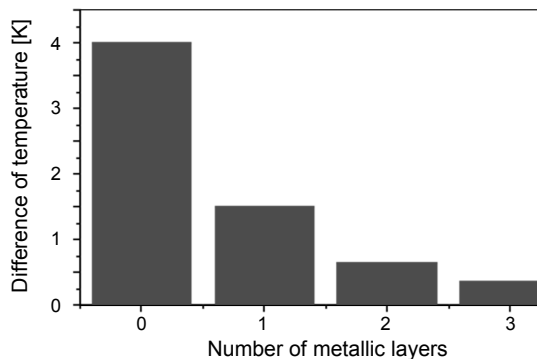


Fig. 5. Difference between maximum and minimum temperature on chamber bottom versus number of metallic layers.

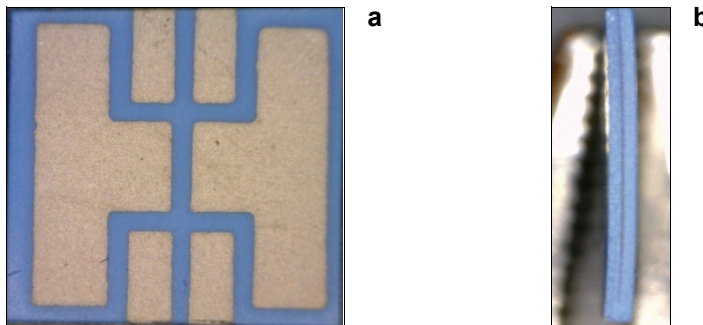


Fig. 6. LTCC test structure with paste DP6146: front view (**a**), and side view (**b**).

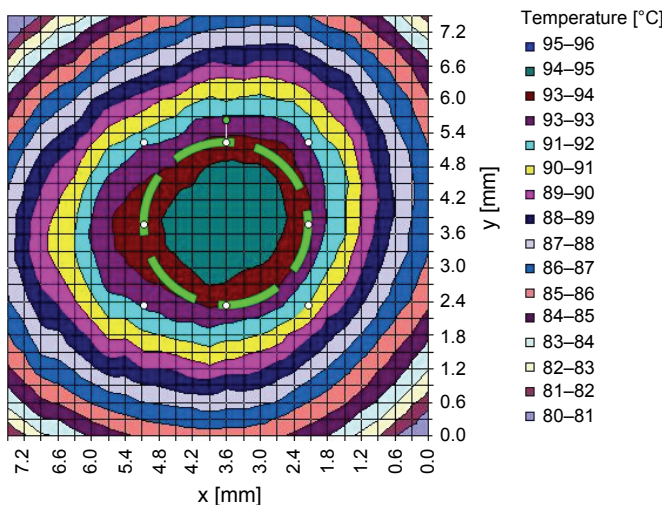


Fig. 7. Map of temperature on the DP951 test structure.

used. The patterns were similar to the scheme showed in Fig. 1. Figure 6 demonstrates the test structure.

The SMD resistor was soldered and a power supply was connected to the structure. The measurement of temperature distribution on the test structure surface was made by an infrared scanner. A map of temperature on the structure is shown in Fig. 7. A location of the chamber bottom was marked in this figure by a green line. The measurement confirmed the results which the authors received in simulation.

4. Manufacturing of PCR microreactor

Based on the results of numerical simulations and temperature distribution measurements, the reactor made of DP951 ceramic with DP6146 ink was proposed. The chamber diameter was 3 mm. The estimated chamber's volume was 6 μl . The dimensions of the chip were 8 mm \times 8 mm \times 1.3 mm. The structure consists of

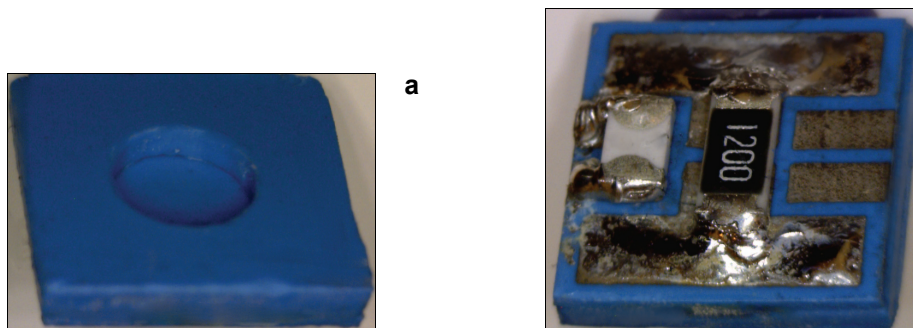


Fig. 8. LTCC microreactor. Top view (a), and bottom view (b).

6 layers of ceramics. The two initial tapes were the basis of the chamber. The layers with metallic pads were constructed similar to the test structure described above.

Nd:YAG laser micromachining and thermocompressive lamination of ceramics were used. The next 4 tapes were laminated together and milled with CNC (computerized numerical control) system. A cold chemical lamination (CCL) was used in order to prevent chamber deformation during technological process. The structure was fired in the air in typical temperature profile for the DP951 ceramics. At the bottom of the chip, a SMD heating resistor in 1206 package and a temperature sensor Pt100 in 0805 package were mounted (Fig. 8).

5. Temperature management system

Proper temperature management is important for PCR process [17]. The ceramic chip was placed in a special design holder and connected to a dedicated electronic temperature control system. A scheme and the photo of the holder is shown in Fig. 9. The programmable electronic system is based on A Tmega168 microcontroller. It enabled heating and temperature measurements. A PID (proportional–integral–derivative) algorithm was used for proper temperature stabilization [18]. A fan was applied to increase convective cooling efficiency. Thus, the time of cooling can be

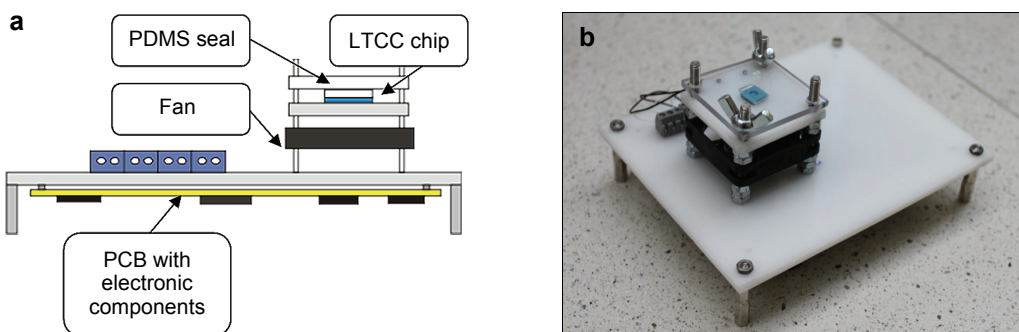


Fig. 9. LTCC chip-based miniaturized PCR system. Scheme (a), photo (b).

decreased. The system was connected to the laptop computer by an USB port. A dedicated software enabled PCR parameters setting and visualization.

6. Biological tests

The PCR was performed using a LIF (laser induced fluorescence) technology. 2 μ M sets of primers (forward – F and reverse – R) were used with F primer labeled by fluorescence dye. Numerous miniSTRs (polymorphisms of mini short tandem repeats) markers were amplified using Qiagen PCR Multiplex Master Mix (Qiagen), according to manufactured protocols under the following temperature profile: (95 °C, 10 min), [(95 °C, 1 min), (57 °C, 1.5 min), (72 °C, 2 min)] \times 30, (72 °C, 10 min), 4 °C forever. Following miniSTRs were amplified: D13S317 (88–132 bp), D3S1358 (72–120 bp), D21S11 (153–211 bp), D16S536 bp), D5S818 (81–117 bp), amylogenin (57 bp female, 57–63 bp male). The expected PCR product sizes differed depending on the alleles distribution. PCR products were separated by capillary electrophoresis (ABI PRISM 310 Genetic Analyzer, Applied Biosystems) together with GeneScan™-LIZ500 Size Standard (Applied Biosystems) and analyzed using Gene Mapper ID v 3.2.1 software. Depending on the fluorescence dye used for F primer labeling, a pick in different color was seen in capillary electrophoresis corresponding to PCR product. Following fluorescence dyes were used: FAM – blue, VIC, HEX – green, ROX – red, NED – black, LIZ – orange. The size was estimated by comparing with GeneScan™-LIZ500 that contained known sizes of DNA fragments from 50 bp up to 500 bp. PCR was successfully performed. Exemplary electrophoregrams with D3S1358 and D5S818 PCR products are shown in Fig. 10. The x axis stands for the fragment size, the y axis corresponds to fluorescence intensity. The area under curve (pick) (AUC) described the PCR efficiency. The forward primer for D3S1358 was labeled by VIC, thus green

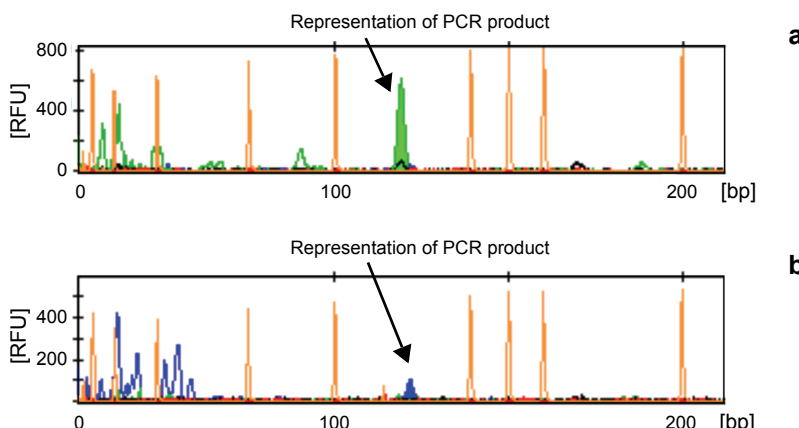


Fig. 10. Example of PCR fragments separation by capillary electrophoresis. PCR performed for D3S1358 (**a**) and for D5S818 (**b**). The lengths of PCR products were assessed comparing to size standard (orange picks). RFU – reference fluorescence unit, bp – base pairs.

pick was visible. On the other hand, the D5S818 forward primer was labeled by FAM, thus a blue pick was visible. The PCR product sizes were assessed by comparing with the size standard containing known fragments. For the presented example, the PCR product sizes were 119 bp and 117 bp for D3S1358 and D5S818, respectively. The unspecific picks around 50 bp were unused during PCR primers. However, PCR products quantity was not satisfied (low AUC). Higher signal picks were expected [11]. In order to improve the PCR efficiency, a special washing solution composed of sulfuric acid and hydrogen dioxide (3:1) was applied for microchip passivation [19]. Nevertheless, it did not considerably improve the PCR results. Further investigation is being performed to increase PCR efficiency.

7. Summary

The research proved that LTCC can be successfully applied as based material for construction of PCR chamber microreactor. Moreover, integration of electronic components was achieved. The construction process was supported by a numerical simulation in order to achieve proper temperature distribution. A metallic layer with high temperature conductivity was buried inside the chip. Uniform temperature distribution on the bottom of the chamber was observed. A dedicated electronic system and holder were constructed. The system proved proper work by successful DNA amplification. The amplification of miniSTR markers was achieved. However, there is still a great need to improve PCR efficiency.

Acknowledgements – This paper has been written as a result of realization of the project entitled *Detectors and sensors for measuring factors hazardous to environment – modeling and monitoring of threats*. The project financed by the European Union via the European Regional Development Fund and the Polish state budget, within the framework of the Operational Programme Innovative Economy 2007–2013. The contract for refinancing No. POIG.01.03.01-02-002/08-00.

The authors also wish to thank the Polish Ministry of Science and Higher Education (grant No. N N515 360336) for financial support.

References

- [1] CORDINGLEY R., KOHAN L., BEN-NISSAN B., PEZZOTTI G., *Alumina and zirconia bioceramics in orthopaedic applications*, Journal of the Australasian Ceramic Society **39**(1), 2003, pp. 20–28.
- [2] NOWAK D., MIŚ E., DZIEDZIC A., KITA J., *Fabrication and electrical properties of laser-shaped thick-film and LTCC microresistors*, Microelectronics Reliability **49**(6), 2009, pp. 600–606.
- [3] MALECHA K., MAEDER T., JACQ C., RYSER P., *Structuration of the low temperature co-fired ceramics (LTCC) using novel sacrificial graphite paste with PVA-propylene glycol-glycerol-water vehicle*, Microelectronics Reliability **51**(4), 2011, pp. 805–811.
- [4] THELEMANN T., FISCHER M., GROß A., MULLER J., *LTCC-based fluidic components for chemical applications*, Proceedings of Ceramic Interconnect and Ceramic Microsystems Technologies – CICMT, April 23–26, 2007, Denver, USA.
- [5] GROß G.A., THELEMANN T., SCHNEIDER S., BOSKOVIC D., KÖHLER J.M., *Fabrication and fluidic characterization of static micromixers made of low temperature cofired ceramic (LTCC)*, Chemical Engineering Science **63**(10), 2008, pp. 2773–2784.

- [6] FERCHER G., HALLER A., SMETANA W., VELLEKOOP M.J., *Ceramic capillary electrophoresis chip for the measurement of inorganic ions in water samples*, Analyst **135**(5), 2010, pp. 965–970.
- [7] FERCHER G., SMETANA W., VELLEKOOP M.J., *Microchip electrophoresis in low-temperature co-fired ceramics technology with contactless conductivity measurement*, Electrophoresis **30**(14), 2009, pp. 2516–2522.
- [8] BEMBNOWICZ P., NOWAKOWSKA D., MAŁODOBRA M., JONKISZ A., DOBOSZ T., GOLONKA L., *The LTCC-glass chip for gel electrophoresis*, Proceedings of 33 International Conference of IMAPS, September 21–24, 2009, Pszczyna, Poland.
- [9] BARTSCH DE TORRES H., RENSCH C., FISCHER M., SCHOBER A., HOFFMANN M., MÜLLER J., *Thick film flow sensor for biological microsystems*, Sensors and Actuators A: Physical **160**(1–2), 2010, pp. 109–115.
- [10] CHUNSHUN ZHANG, JINLIANG XU, WENLI MA, WENLING ZHENG, *PCR microfluidic devices for DNA amplification*, Biotechnology Advances **24**(3), 2006, pp. 243–284.
- [11] BEMBNOWICZ P., MAŁODOBRA M., KUBICKI W., SZCZĘPAŃSKA P., GÓRECKA-DRZAZGA A., DZIUBAN J., JONKISZ A., KARPIEWSKA A., DOBOSZ T., GOLONKA L., *Preliminary studies on LTCC based PCR microreactor*, Sensors and Actuators B: Chemical **150**(2), 2010, pp. 715–721.
- [12] CHOU C., CHAGRANI R., ROBERTS P., SADLER D., BURDON J., ZENHAUSERN F., LIN S., MULHOLLAND A., SWAMI N., TERBRUEGGEN R., *A miniaturized cyclic PCR device-modeling and experiments*, Microelectronic Engineering **61–62**, 2002, pp. 921–925.
- [13] ZAWADA T., *Simultaneous estimation of heat transfer coefficient and thermal conductivity with application to microelectronic materials*, Microelectronics Journal **37**(4), 2006, pp. 340–352.
- [14] MARKOWSKI P., DZIEDZIC A., *Numerical simulations of temperature distribution inside thermopiles*, Proceedings of International Conference MIDEM 2009, Postojna, Slovenia, pp. 161–166.
- [15] SADLER D.J., CHAGRANI R., ROBERTS P., CHOU C.F., ZENHAUSERN F., *Thermal management of BioMEMS*, Proceedings of The Eighth Intersociety Conference on Thermal and Thermomechanical Phenomena in Electronic Systems, 2002, San Diego, USA.
- [16] www.ansys.com, 18.02.2011.
- [17] SADLER D.J., CHAGRANI R., ROBERTS P., CHIA-FU CHOU, ZENHAUSERN F., *Thermal management of BioMEMS: Temperature control for ceramic-based PCR and DNA detection devices*, IEEE Transactions on Components and Packaging Technology **26**(2), 2003, pp. 309–316.
- [18] BEMBNOWICZ P., NOWAKOWSKA D., GOLONKA L., *Integrated LTCC chamber with optical ports and thermal control elements*, Proceedings of 32nd International Spring Seminar on Electronics Technology, May 13–17, 2009, Brno, Czech Republic.
- [19] RADSTROM P., KNUTSSON R., WOLFFS P., LOVENKLEV M., LOFSTROM C., *Pre-PCR processing. Strategies to generate PCR-compatible samples*, Molecular Biotechnology **26**, 2004, pp. 133–146.

Received September 25, 2010